Yang, G., Zomorodian, M., Belarbi, A. & Ayoub, A. (2016). Uniaxial Tensile Stress-Strain Relationships of RC Elements Strengthened with FRP Sheets. Journal of Composites for Construction, 20(3), doi: 10.1061/(ASCE)CC.1943-5614.0000639

UNIAXIAL TENSILE STRESS STRAIN RELATIONSHIPS OF RC ELEMENTS STRENGTHENED WITH FRP SHEETS

Guang Yang[1], Mehdi Zomorodian[2], Abdeldjelil Belarbi[3], Ph.D., P.E.,

and Ashraf Ayoub[4], Ph.D., P.E.

[1]Ph.D. Candidate, Department of Civil and Environmental Engineering, University of Houston, Houston, USA (corresponding author). E-mail: gyang@central.uh.edu

[2]Ph.D. Candidate, Department of Civil and Environmental Engineering, University of Houston, Houston, USA. E-mail: szomorodian@uh.edu

[3]Hugh Roy and Lillie Cranz Cullen Distinguished Professor, Department of Civil and Environmental Engineering, University of Houston, Houston, USA. E-mail: belarbi@uh.edu

[4]Professor and Royal Academy of Engineering Pell Frischmann Chair, Department of Civil Engineering, City University London, London, UK.
E-mail: ashraf.ayoub.1@city.ac.uk

ABSTRACT

The behavior of Fiber-Reinforced Polymer strengthened Reinforced Concrete (FRP RC) members under shear is still not fully understood due to the complexity associated with the behavior. The main reason is the lack of accurate stress strain relationships for the components constituting the composite members. This paper presents the experimental and analytical investigations of stress strain relationships of concrete and steel in FRP RC members under uniaxial tension. These stress strain relationships are required in the equations of the softened truss model theory to predict the shear behavior of the FRP RC element. Thirteen full scale FRP RC prismatic specimens with different FRP, steel reinforcements and FRP wrapping schemes were tested. The results show that the tensile behavior of the concrete and steel was altered due to the externally bonded FRP sheets. Modified analytical expressions were proposed taking into account the interaction between the materials. Moreover, as a key issue in serviceability, the crack spacing

and crack width were also presented. The observed results were compared with the existing code provisions.

KEYWORDS: FRP; uniaxial tensile loading; reinforced concrete; stress strain relationships; crack spacing; crack width

1. INTRODUCTION

Fiber-Reinforced Polymer (FRP) materials have being widely used in civil engineering applications for more than three decades. Well established analytical models are already available for FRP strengthened beams and columns under flexural and axial loadings. However, the behavior of such members under shear stress field is still under investigation due to the high level of complexity associated with the shear behavior (Zararis 2003). Most of the available analytical models for predicting the shear behavior of FRP RC members resulted in relatively large discrepancies when compared to experimental results (Belarbi et al. 2011). The most important reason for this is the lack of accurate stress strain relationships for FRP RC elements. In the previous developed models and design codes, the shear contributions of concrete, internal steel reinforcements and externally bonded FRP reinforcements were derived independently. However, the high level of interaction between these materials should be considered (Bousselham and Chaallal 2008; Chen et al. 2010). To accurately predict the behavior of FRP RC elements in shear, the stress - strain relationships of each component and the interactions among them have to be carefully investigated.

Stress - strain relationships of concrete, steel and FRP in tension are required in the equations of theories needed to predict the behavior of the FRP RC element under shear. It has been observed by several researchers that the presence of the externally bonded FRP typically alters the crack patterns and bond condition of the member under uniaxial tensile load, which leads to the change of the main characteristics of the stress - strain relationships of concrete and steel reinforcements (Ueda et al. 2002; Ceroni et al. 2004; Farah and Sato 2011). In this paper, these stress - strain relationships were studied by testing thirteen full-scale FRP RC prismatic specimens. On the basis of the stress - strain relationships in Softened Membrane Model (SMM), the modified

mathematical expressions for concrete and steel in uniaxial tension were proposed. The effects of the FRP reinforcement ratio, steel reinforcement ratio, and the wrapping scheme were studied. Although most frequently neglected by researchers, shrinkage of concrete was identified as another important factor that affects the tensile behavior of the member (Bischoff 2001; Kaklauskas et al. 2009; Kaklauskas and Gribniak 2011). In this paper, shrinkage has been considered in the derivation of the stress - strain relationships.

Moreover, as a key issue to warrant the functionality of the FRP RC members in serviceability state, the knowledge of crack spacing and crack width is still not fully developed (Ceroni and Pecce 2009). Several codes provide formulas to calculate crack width for RC elements in serviceability conditions, including EC2-04, ACI 318-95, JSCE 2001, and CSA 2004. However, limited resources are available for the crack width and spacing predictions in design codes for FRP - strengthened RC structures (Lee et al. 1999; Sato et al. 1999; Yoshizawa et al. 1999; Tripi et al. 2000; Matthys 2000; Ueda et al. 2002; Ceroni and Pecce 2009). The only available code formula for the prediction of mean crack spacing and width in FRP - strengthened RC members is presented in fib Bulletin 14 (fib 14 2001), which is based on the work presented by Matthys (2000). In this paper, the crack spacing and width were captured by a digital image correlation (DIC) system, ARAMIS (GOM MbH., Germany). The comparison between experimental results and the predictions from several codes and provisions are presented and discussed.

2. EXPERIMENTAL PROGRAM

Thirteen full-scale FRP RC specimens were tested under uniaxial tensile loading. Fig. 1 presents the test setup and dimensions of the specimens. The specimens were 1397 mm long prisms with a cross section of 257 mm × 178 mm. The rebar was welded onto a pre-embedded connector insert that was bolted to a connector yoke. At each end of the specimen, two hydraulic actuators with a

total capacity of 1780 kN were used to apply tensile loading to the specimens through the pin connections on the connector yokes. FRP sheets with a width of 203 mm were applied on two opposite sides of the specimen. To prevent the premature failure at the loading zone, several confining plates were installed at the end region of the specimen. Two Linear Variable Differential Transformers (LVDTs) were installed on North and South side to measure the average deformation of the specimen. In order to monitor the effect of bending, two additional LVDTs were installed on the top and bottom surface of the specimen. Strain Gauges (SG) were applied on the rebar and FRP sheets to monitor the local strains along these materials.

Three different wrapping schemes were used, including Side Bond (SB), Fully Wrap (FW) and U-wrap with FRP Anchors (FA), as shown in Fig. 2a-2c. For simplicity, U-wrap with FRP anchor was referred to as FRP Anchor (FA) in this paper. The FRP anchor was fabricated by a bundle of the same carbon fiber as the FRP sheets to provide compatibility between the materials used. After saturating the FRP anchor into epoxy resin, one end of the anchor was inserted through a pre-drilled hole on the concrete surface, and the fibers on the other end were then fanned out on top of the FRP sheet as shown in Fig. 2c.

Standard material tests were conducted to obtain the mechanical properties. Type III cement was used for concrete casting, standard 152 mm × 305 mm cylinders were tested under compression as per ASTM C39. Grade 60 ASTM A706 low-alloy steel deformed bars were used as internal reinforcements. The FRP sheets were made of unidirectional carbon fibers with the material properties determined from coupon tests according to ASTM D3039. The wet lay-up system was used for installation of FRP sheets. The specimen was grinded, sandblasted and power washed to provide proper concrete surface conditions that would develop the necessary bond strength between the concrete and FRP sheets. Putty and primer were applied first on the surface, the

sheets were then impregnated by epoxy resin and applied in-situ. Specimens were then cured at least 72 hours before testing. Pull-off tests were carried out to verify proper bond strength as per ASTM D7522. The tensile strength σ_p obtained from the pull-off tests shall be at least 1.4 MPa as per ACI 440.2R-08. Details of the material properties are presented in Table 1. The specimens are identified by steel rebar sizes (#3, #4, #5), FRP thicknesses (0.6 mm and 1 mm, i.e., 0.025 in and 0.040 in), and wrapping schemes (Fully Wrap, Side Bond, U-wrap with FRP Anchor). As an example: S4-025-SB stands for the specimen with #4 rebar, 0.6 mm (0.025 in) thick FRP sheet and Side Bond wrapping scheme method. REF-R3/R4/R5 are reference specimens with #3, #4 and #5 rebars respectively. The shrinkage strains for concrete and steel reinforcements in each specimen were also shown in Table 1, the details of the calculation are presented in the following section.

A digital image correlation (DIC) system, ARAMIS (GOM MbH., Germany) was used to obtain the displacement and deformation field on one side of the specimen. Through this DIC-based non-contact measurement system, the crack spacing and crack width of the specimen were captured in real time. Load was measured with the load cells installed on each hydraulic actuator. Testing initially started using load control up to first cracking and then switched to displacement control until failure of the specimen.

3. AVERAGE STRESS STRAIN RELATIONSHIP OF CONRETE IN TENSION

The applied tensile force P is resisted by concrete, steel and externally bonded FRP sheets. In the pre-cracking stage, steel, FRP, and concrete are elastic. The cracking strength of concrete is determined by:

$$f_{cr} = \frac{P_{cr}}{A_c} - \rho_s E_s \varepsilon_{cr} - \rho_f E_f \varepsilon_{cr} \quad (1)$$

where ρ_s and ρ_f are the reinforcement ratios of steel and FRP, respectively; E_s and E_f are the modulus of elasticity of steel and FRP, respectively; ε_{cr} is the cracking strain in the specimen and P_{cr} is the cracking load; A_c is the gross area of the cross-section. It was found that the best expressions that fit the test results are:

$$f_{cr} = 0.3\sqrt{f_c'(\text{MPa})} \quad (2)$$

$$E_c = 3900\sqrt{f_c'(\text{MPa})} \quad (3)$$

These equations were first proposed by Belarbi and Hsu (1994). Fig. 3 shows the comparison between the experimental results and Eqns. (2) and (3).

In the post-cracking stage, the stress distribution along the length of the member was altered. At the crack location, the tensile stress was carried only by FRP and steel. Between the cracks, the tensile stress was transferred to concrete gradually through the bond action between concrete and reinforcements (steel and FRP). Since the concrete cracked at a lower level of strain, the steel and FRP are still in the elastic range and therefore the calculations of average stresses are given as follows:

$$\sigma_s = E_s \frac{1}{L}\int_0^L \varepsilon_s(x)\,dx = E_s \varepsilon_1 \quad (4)$$

$$\sigma_f = E_f \frac{1}{L}\int_0^L \varepsilon_f(x)\,dx = E_f \varepsilon_1 \quad (5)$$

where σ_s and σ_f are the average stresses of steel and FRP, respectively; $\varepsilon_s(x)$ and $\varepsilon_f(x)$ are the local strains for steel and FRP at a distance x from the crack, respectively; ε_1 is the average strain of the member (considering the crack width); L is the length between two cracks.

Hence, the total applied tensile load

$$P = (\rho_s E_s \varepsilon_1 + \rho_f E_f \varepsilon_1 + \sigma_c) / A_c \tag{6}$$

Average stress in concrete can then be calculated from Eqn. (6) as:

$$\sigma_c = \frac{P}{A_c} - \rho_s E_s \varepsilon_1 - \rho_f E_f \varepsilon_1 \tag{7}$$

In this paper, the short-term (creep effect insignificant) shrinkage effect was considered using the approach proposed by Kaklauskas and Gribniak (2011). A fictitious axial force was proposed to evaluate the effect of the shrinkage on the specimen. Based on this approach, the shrinkage strains in the concrete and steel can be expressed as:

$$\varepsilon_{c,sh} = \frac{\varepsilon_{sh} E_s A_s}{E_c A_c + E_s A_s} \tag{8}$$

$$\varepsilon_{s,sh} = \frac{\varepsilon_{sh} E_c A_c}{E_c A_c + E_s A_s} \tag{9}$$

where ε_{sh} is the shrinkage strain in a plain concrete specimen. Gribniak (2009) suggested to calculate the initial shrinkage strain ε_{sh} of concrete by Eurocode 2 method. The same approach was applied in this paper to account for the effect of shrinkage for each specimen. Details of the shrinkage strain are presented in Table 1.

3.1 Experimental results for concrete in tension

With the load P and the average strain ε_1 measured from the test, the average stress strain relationships of concrete in tension were obtained, see Fig. 4. The average stress σ_c was normalized by the tensile strength f_{cr} of the specimen.

Fig. 4a and 4b indicate that the FRP reinforcement enhanced the descending portion of the stress strain curve when compared to the reference specimen. It could be also stated that the increase in tension stiffening is more significant in specimens with lower FRP reinforcement ratio. Similar conclusions were also put forward by other researchers (Farah and Sato 2011) and explained as below: the average concrete stress is developed by bond actions between concrete and the reinforcements (FRP and steel). When the specimen is strengthened with smaller amount of FRP, the bond stress between FRP and concrete increases while the bond stress between steel and concrete decreases, the increase of the FRP bond is dominant so the tension stiffening increases compared to un-strengthened RC elements; when the amount of FRP reinforcements increases, the crack spacing decreases, which caused a greater deterioration of steel bond, this deterioration becomes dominant and caused a decrease of tension stiffening of concrete. The same phenomenon was also observed in the author's tests that the crack spacing decreases with the increase of the FRP reinforcement ratio; detail information of cracks is presented in the following section of this paper. Fig. 4c and 4d show that the tension stiffening is more evident in specimen strengthened with fully wrap method than FRP anchor and side bond. This could be attributed to the greater increase of the bond action between FRP sheets and concrete with fully wrap as compared to the cases with FRP anchor and side bond. It was also observed from Fig. 4e and 4f that the enhancement of descending portion due to FRP is slightly more significant in the specimens with higher internal reinforcement ratio.

3.2 Proposed equations for concrete in tension

On the basis of the test results, mathematical expressions for concrete in tension were proposed, see Eqns. (10) and (11).

$$\sigma_c = E_c \varepsilon_1 \qquad \text{when } \varepsilon_1 \le \varepsilon_{cr} \tag{10}$$

$$\sigma_c = f_{cr} \left(\frac{\varepsilon_{cr}}{\varepsilon_1} \right)^{\alpha_f} \qquad \text{when } \varepsilon_1 > \varepsilon_{cr} \tag{11}$$

The chosen format of the tension stiffening model was first proposed by Tamai et al. (1987) and verified by Belarbi and Hsu by testing 17 large scale RC panels (1994), α_f was determined to be 0.4 for un-strengthened RC elements. Based on the results in previous section, α_f was assumed to have a format as:

$$\alpha_f = K_w K_{f/s} \tag{12}$$

where K_w and $K_{f/s}$ are two factors considering the effects of wrapping scheme and FRP/steel stiffness ratio, respectively.

With mathematical regression of the test results using the proposed format in Eqn. (11), the experimental values of $\alpha_{f,exp}$ were obtained. The relationships between $\alpha_{f,exp}$ and the wrapping scheme as well as the FRP/steel stiffness ratio are shown in the Fig. 5a and 5b. For simplicity, K_w was assumed to be 0.9, 1 and 1.6 for FW, FA and SB wrapping scheme, as shown in Eqn. (13). By regression of the result shown in Fig. 5b, $K_{f/s}$ was found to best fit Eqn. (14). The comparison of $\alpha_{f,exp}$ and the predictions of Eqn. (11)-(14) is shown in Fig. 5c.

$$K_w = \begin{cases} 1.6, & \text{Side Bond} \\ 1, & \text{FRP Anchor} \\ 0.9, & \text{Fully Wrap} \end{cases} \tag{13}$$

$$K_f = 0.25\left(\frac{\rho_f E_f}{\rho_s E_s}\right) + 0.15 \tag{14}$$

The value of K_w is assigned to describe the effect of different wrapping schemes, as shown in Fig. 4c and 4d. As for $K_{f/s}$, it can be observed from Fig. 5b that the proposed equation was verified in the range where $\rho_f E_f / \rho_s E_s$ is between 0.25 and 1.11. The verification of the boundary value for the proposed equation requires more test results. Fig. 6 shows the comparison between some test results and the proposed equations. An acceptable level of agreement was observed.

4. AVERAGE STRESS STRAIN RELATIONSHIP OF STEEL IN TENSION

The stress strain curve of the steel embedded in concrete is quite different than that of a bare rebar; a reduction of yielding stress was observed by several researchers (Okamura et al. 1985; Shima et al. 1987; Tamai et al. 1987; Belarbi and Hsu 1994). Belarbi and Hsu proposed a simplified bilinear expression as shown in Eqn. (15)-(20). A so-called apparent yield stress f_y' was proposed to describe the reduction of yielding stress.

$$f_s = E_s \varepsilon_s \qquad \varepsilon_s < \varepsilon_y' \tag{15}$$

$$f_s = (0.91 - 2B)\, f_y + (0.02 + 0.25B)\, E_s \varepsilon_s \qquad \varepsilon_s \geq \varepsilon_y' \tag{16}$$

$$\varepsilon_y' = f_y' / E_s \tag{17}$$

$$f_y^{'} = (0.93 - 2B)\, f_y \tag{18}$$

$$B = \frac{1}{\rho_s}\left(\frac{f_{cr}}{f_y}\right)^{1.5} \tag{19}$$

$$f_{cr} = 0.31\sqrt{f_c^{'}(\text{MPa})} \quad \text{and} \quad \rho_s \geq 0.15\% \tag{20}$$

The comparison between the stress strain relationships of steel in FRP RC element and those of bare rebars is shown in Fig. 7a-7c. The results show that the apparent yielding stress was altered due to the existence of the FRP. It can also be observed that the difference between the yield stress of bare rebar and apparent yield stress becomes smaller with the increase of FRP stiffness. This effect is more evident for #3 rebar compared with #4 and #5 rebar. This can be explained that in the specimen with a smaller internal steel reinforcement ratio, the FRP tends to work more effectively in crack width control. As a result, the local yielding of the rebar at the crack location was postponed, which leads to an increase of the apparent yield stress. Based on this phenomenon, the steel reinforcement ratio ρ_s in Eqn. (19) was proposed to be replaced by a new ratio called equivalent reinforcement ratio ρ_e, which considered the contribution of FRPs. The following equations were proposed to calculate ρ_e:

$$\rho_e = \rho_s + n_f \rho_f \tag{21}$$

$$n_f = \frac{E_f}{E_s} \tag{22}$$

Fig. 8 shows the comparison between the proposed equations and the test results. Since #4 and #5 rebar have no yielding plateau, the stiffness of the post-yielding portion for the specimen with

#4 and #5 rebar was considered same as the post-yielding stiffness of the respective bare rebar. Fig. 8 shows an acceptable level of agreement between the proposed model and the test results.

5. COMPARISON OF THE LOAD STRAIN CURVES

To validate the proposed stress - strain relationships of concrete and steel in tension, comparison of the load strain curves between the proposed model and test results was shown in Fig. 9. It can be observed that the model predicted the load - strain curve quite well.

6. CRACK SPACING AND CRACK WIDTH

At serviceability conditions, in addition to the stress transfer between steel rebar and the surrounding concrete, the stress transfer between the externally bonded FRP sheet and the concrete substrate significantly modifies the cracking behavior. Also, the number of cracks and crack spacing change, depending on the bond behavior at the concrete-FRP interface (Smith and Teng 2002), i.e. if number of cracks increases, crack spacing decreases and therefore crack width decreases. The development of cracks is progressive and as the load increases new cracks will form until a stabilized cracking condition is reached. At this stage, no new cracks will develop because the tensile stress in concrete between two cracks is smaller than the tensile strength of concrete (Ceroni et al. 2004). In this paper, the crack characteristics including crack width, number of cracks, and spacing were all monitored and measured using a DIC system (ARAMIS) at the conducted experiments.

In FRP RC members, average crack widths are generally smaller than for un-strengthened members at the same smeared strain level (Fig. 10), due to the additional bond action developing at the FRP-concrete interface which reduces the crack spacing. As shown in Fig. 10, fully wrap and U-wrap with FRP anchor wrapping schemes provide better control of crack width as

compared to side bonding. Furthermore, the thinner FRP (0.6mm, 0.025 in) provides better crack control compared to the thicker FRP (1mm, 0.04 in). It can be concluded that the fully wrap method with thinner FRP shows a better behavior in terms of crack control compared to the other wrapping schemes and FRP thicknesses. As shown previously, the same conclusion was reached in terms of tension stiffening.

Generally, it is assumed that all the deformation of the member when a crack is formed is accommodated in that crack. The crack width is primarily a function of the deformation of the reinforcement and concrete between two adjacent cracks (fib 40 2007). When all cracks have formed, the crack width is given by the following relationship, which is based on compatibility:

$$w = S_{rm}\varepsilon_m \tag{23}$$

Where w is the average crack width; S_{rm} is the average crack spacing and ε_m is the average strain. In this paper, the available code guidelines for crack spacing in RC members, EuroCode EC2-92 (1992), EuroCode EC2-04 (2004) and for FRP RC members, fib14 (2001) are reviewed in order to determine their accuracies for RC elements strengthened with FRP sheets. To calculate the crack spacing in RC members, EC2-92 (1992) proposed the following equation:

$$S_{rm} = 50 + 0.25K_1K_2\frac{\phi}{\rho_{eff}} \tag{24}$$

Where K_1 is the bond coefficient equal to 0.8 for deformed bars and 1.6 for plain bars; K_2 is the coefficient to take into account the type of loading equal to 0.5 for bending and 1.0 for pure tension; ϕ is the diameter of steel bar; and ρ_{eff} is the effective reinforcement ratio.

In EC2-04 (2004) the following equation was proposed to evaluate the maximum crack spacing for RC elements:

$$S_{r,max} = 3.4c + 0.425K_1K_2\frac{\phi}{\rho_{eff}} \tag{25}$$

Where c is the concrete cover and K_1, K_2, ϕ, and ρ_{eff} are defined same as in EC2-92 (1992). It was found experimentally that a reasonable estimate of the characteristic crack width is obtained if the maximum crack spacing is assumed to be 1.7 times the average crack spacing (EC2-04). Therefore, based on EC2-04, the average crack spacing, S_{rm}, can be calculated as follows:

$$S_{rm} = 2c + 0.25K_1K_2\frac{\phi}{\rho_{eff}} \tag{26}$$

Ceroni et al. (2004) proposed the following expression to consider the effect of externally bonded FRP in EC2 equations:

$$\rho_{eff} = \frac{A_s + A_f E_f / E_s}{A_{c,eff}} \tag{27}$$

Where A_s is the area of steel reinforcement; A_f is the area of the FRP reinforcement; E_f and E_s are the Young's modulus of FRP and steel respectively; $A_{c,eff}$ is the effective area of concrete in tension.

The following equation was presented in fib 14 (2004) to calculate the average crack spacing in RC members strengthened with FRP sheets or laminates.

$$S_{rm} = \frac{2 f_{ctm} A_{c,eff}}{\tau_{sm}u_s + \tau_{fm}u_f} \tag{28}$$

Where f_{ctm} is the mean tensile strength of concrete, u_s and u_f are the perimeters of the steel bar and FRP sheets bonded to concrete, $\tau_{fm} = 1.8\, f_{ctm}$ (CEB-FIP Model Code 1990) and $\tau_{sm} = 1.25\, f_{ctm}$ (Holzenkampfer 1994) are the bond stresses along the concrete-steel interface and concrete-FRP interfaces, which are assumed constant.

The experimental results of the tests presented herein, are compared with the aforementioned code guidelines in terms of crack spacing in order to review their effectiveness. In Fig. 11. The experimental values of mean crack spacing, $S_{rm,exp}$, are compared with the design values provided by EC2-92 (1992), EC2-04 (2004) and fib14 (2001).

In order to assess the reliability of the code predictions, the mean percentage of deviation, σ%, the average ratio of code predictions to experimental results, δ, the standard deviation of variable δ, Coefficient of determination, R^2, and correlation coefficient, r, are shown in Table 2.

The statistical parameters reported in Table 2 show that for crack spacing the code guidelines of EC2-04 and fib 14 present a larger scatter compared to the EC2-92 prediction. The mean variable of parameter δ equal to 0.89 and 0.88 for EC2-92 and EC2-04 respectively, shows the underestimation of the experimental results. As in fib 14, δ equals 1.12, which shows the overestimation of the experimental results. Also, evaluating the R^2 and r values for EC2-92 compared to EC2-04 and fib 14 shows that EC2-92 predictions show a better agreement with the experimental results. The R^2 value for fib 14 equals -26.23, which shows that the prediction are very scatter compared to the Euro Code guidelines. This can be due to the fact that in fib 14 predictions, the FRP reinforcement ratio is not considered as an effecting parameter.

Although the EC2-92 formulation, compared to the EC2-04 and fib 14 guidelines, for crack

spacing shows a better prediction in FRP RC members, further research is necessary in order to have a more accurate prediction of the crack spacing and ultimately crack widths. The main parameters influencing the development of cracks such as rebar diameter, effective area of concrete, concrete cover, FRP reinforcement ratios, and parameters such as wrapping scheme should be considered in the development of a new expression for the prediction of crack spacing and crack width.

7. CONCLUSIONS

This paper presented the experimental and analytical investigations of the stress - strain relationships of steel and concrete in FRP RC element under uniaxial tension load. The main conclusions are as follows.

- The existence of FRP enhances the tension stiffening effect of concrete in FRP RC element. The magnitude of the increase is affected by the FRP/steel reinforcement ratio and the wrapping scheme.
- The apparent yielding stress was altered due to the externally bonded FRPs. The difference between the yield stress of bare rebar and apparent yield stress becomes smaller with the increase of FRP stiffness.
- Mathematical expressions were proposed for both concrete and steel in tension taking into account the interaction between the materials. The proposed equations provide an acceptable prediction when compared to the experimental results.
- The EC2-92 formulation, compared to other guidelines for crack spacing, shows a better prediction in FRP RC members. Further research is necessary in order to have a more accurate prediction of the crack spacing and ultimately crack widths, considering all the main

parameters which affect the cracking phenomena in such members.

ACKNOWLEDGEMENTS

This research was supported by the National Science Foundation, award number 1100930. Steel reinforcement and FRP materials are donation from GERDAU AMERISTEEL Co. and FYFE. Co, respectively. Their support is greatly acknowledged.

REFERENCES

1. ACI (American Concrete Institute). (1995). "Building Code Requirements for Structural Concrete." ACI 318-95, Detroit, MI.

2. ACI (American Concrete Institute). (2008). "Guide for the design and construction of externally bonded FRP systems for strengthening concrete structures." ACI 440.2R-08, Farmington Hills, MI.

3. Belarbi, A., and Hsu, T. T. C. (1994). "Constitutive laws of concrete in tension and reinforcing bars stiffened by concrete." ACI Structural Journal, 91(4), 465-474.

4. Belarbi, A., Bae, S. W., Ayoub, A., Kuchma, D., Mirmiran, A., and Okeil, A. (2011). National Cooperative Highway Research Program (NCHRP) Report 678: Design of FRP Systems for Strengthening Concrete Girders in Shear, Washinton D.C..

5. Bischoff, P. H. (2001). "Effects of shrinkage on tension stiffening and cracking in reinforced concrete." Canadian Journal of Civil Engineering, 28(3), 363-374.

6. Bousselham A., and Chaallal O. (2008). "Mechanisms of shear resistance of concrete beams strengthened in shear with externally bonded FRP." Journal of Composite for Constructions, 12(5), 499-512.

7. CSA (Canadian Standard Associations). (2004). "S474 concrete structures." Mississauga, Ontario, Canada

8. CEB (European Committee for Standardization). (1993), "CEB-FIP Model Code 1990, Design Code." Lausanne, Switzerland, Thomas Telford.

9. CEN. Eurocode 2 (1992). "Design of concrete structures – Part 1-1: General rules and rules

for buildings", ENV 1992-1-1: 1991.

10. CEN. Eurocode 2 (2004). "Design of concrete structures – Part 1-1: General rules and rules for buildings", EN 1992-1-1E.

11. Ceroni, F., Pecce M., and Matthys, S. (2004). "Tension stiffening of RC ties strengthened with externally bonded FRP sheets." Journal of Composites for Construction, 8(1), 510-518.

12. Ceroni, F., and Pecce, M. (2009). "Design provisions for crack spacing and width in RC elements externally bonded with FRP." Composites: Part B, 40, 17-28.

13. Chen G. M., Teng J. G., and Chen J. F. (2010). "Interaction between steel stirrups and shear-strengthening FRP strips in RC Beams." Journal of Composite for Constructions, 14(5), 498-509.

14. Farah, Y., and Sato, Y. (2011). "Uniaxial tension behavior of reinforced concrete members strengthened with carbon fiber sheets." ASCE Journal of Composites for Construction, 15(2), 215-228.

15. Fib Bulletin 14 (2001). "FRP as externally bonded reinforcement of R.C. structures: basis of design and safety concept", TG9.3.

16. Fib Bullettin 40 (2007). "FRP reinforcement in R.C. structures, TG9.3.

17. Gribniak, V. (2009). "Shrinkage influence on tension-stiffening of concrete structures." Doctoral thesis, Vilnius Gediminas Technical University.

18. Holzenkampfer P. (1994). "Ingenieurmodelle des Verbunds geklebter bewehrung fur Betonbauteile", PhD Thesis, Technical University Braunschweig, Germany.

19. Japan Society of Civil Engineers (JSCE). (2001). "Standard Specifications for Concrete Structures−Maintenance." Tokyo, 170.

20. Kaklauskas, G., Gribniak, V., Bacinskas, D. and Vainiunas, P. (2009). "Shrinkage influence on tension stiffening in concrete members." Engineering Structures, 31(6), 1305-1312.
21. Kaklauskas, G. and Gribniak, V. (2011). "Eliminating shrinkage effect from moment-curvature and tension-stiffening relationships of reinforced concrete members." Journal of Structural Engineering, 137(12), 1460-1469.
22. Lee, Y. J., Boothby, T. E., Bakis, C. E., and Nanni, A. (1999). "Slip modulus of FRP sheets bonded to concrete." Journal of Composites for Construction, 3(4), 161-167.
23. Matthys, S. (2000). "Structural behaviour and design of concrete members strengthened with externally bonded FRP reinforcement." PhD thesis, Gent University.
24. Okamura, H., Maekawa, K., and Sivasubramaniyam, S. (1985). "Verification of modeling for reinforced concrete finite element." Proceedings of Japan-US Seminar on Finite Element Analysis of Reinforced Concrete Structures, Tokyo, ASCE, 528-543.
25. Sato, Y., Shouji, K., Ueda, T., and Kahuta, Y. (1999). "Uniaxial Tensile Behavior of Reinforced concrete elements Strengthened by Carbon Fiber Sheet." Proc. Of Fourth Int. Symposium on FRP Reinforcement, ACI, 697-710.
26. Shima, H., Chou, L., and Okamura, H. (1987). "Micro and macro models for bond in reinforced concrete." J. Fac. Engrg. Univ. Tokyo Ser. B, 39 (2), 133-194
27. Smith, S. T., and Teng, J. G. (2002). "FRP-strengthened RC beams. I: Review of debonding strength models." Engineering Structures, 24(4), 385-95.
28. Tamai, S., Shima, H., Izumo, J. and Okamura, H. (1987). "Average stress-strain relationship in post yield range of steel bar in concrete." Concrete Library of JSCE, 11, 117-129. (Translation from Proceedings of JSCE, No. 378/Vol. 6, February 1987).
29. Tripi, J. M., Bakis, C. E. Boothby, T. E., and Nanni, A. (2000). "Deformation in concrete

with external CFRP sheet Reinforcement." Journal of Composites for Construction, 4(2), 85-94.

30. Ueda, T., Yamaguchi, R., Shoji, K., and Sato, Y. (2002). "Study on behavior in tension of reinforced concrete members strengthened by carbon fiber sheet." J. Compos. Constr., 6(3), 168-174.
31. Yoshizawa, H., and Wu, Z. (1999). "Crack Behavior of Plain Concrete and Reinforced Concrete Members Strengthened with Carbon Fiber Sheets." Proc. of Fourth Int. Symposium on FRP Reinforcement, ACI, 767-779.
32. Zararis, P. D. (2003). "Shear Strength and Minimum Shear Reinforcement of Reinforced Concrete Slender Beams." ACI Structural Journal, 100(2), 203-214.

Figures

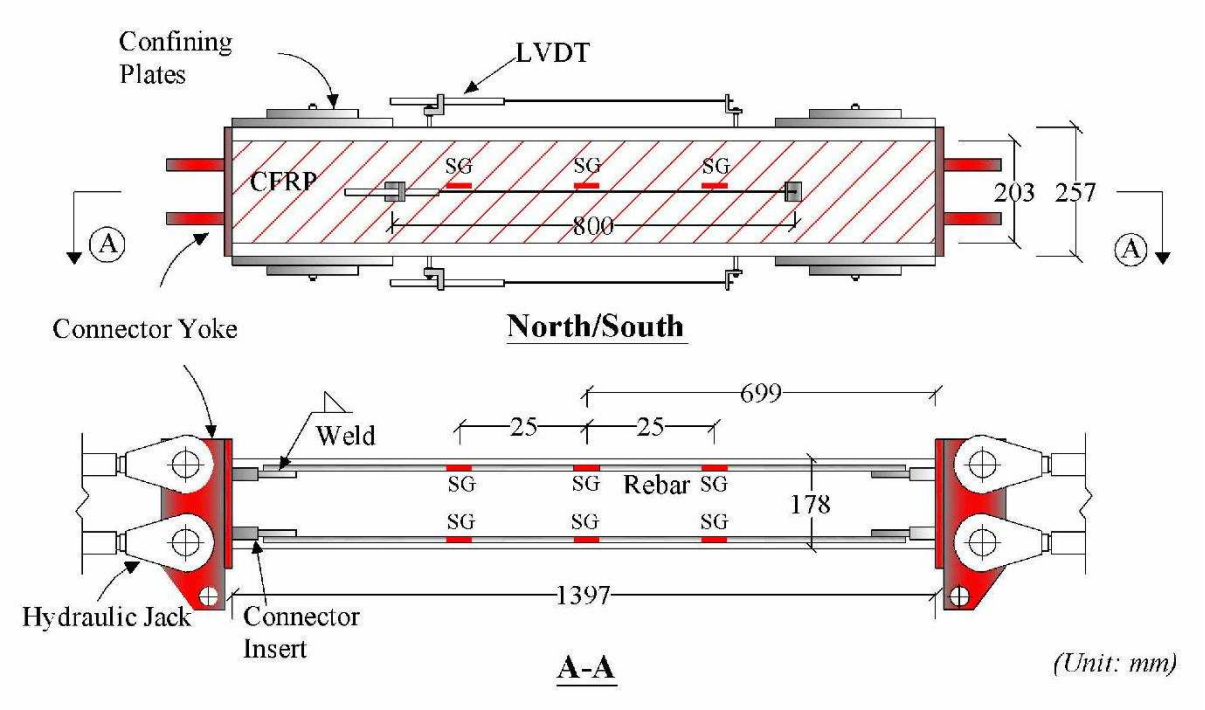

Fig. 1. Test setup and specimen layout

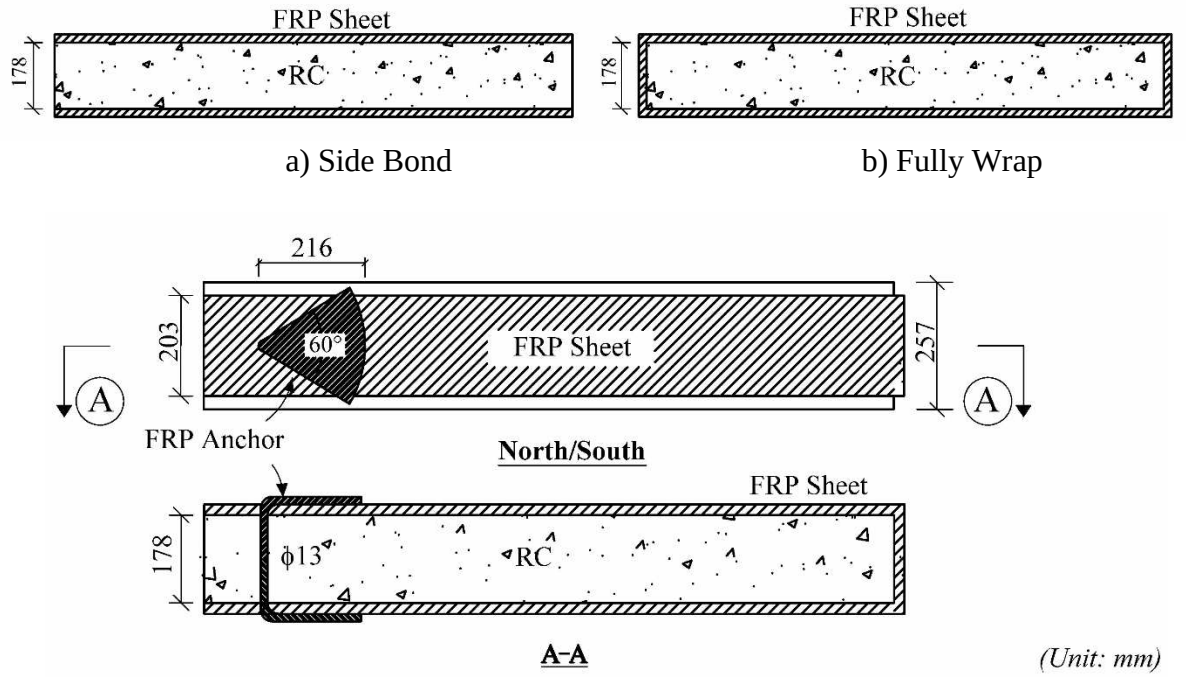

Fig. 2. Wrapping scheme and anchorage system detail

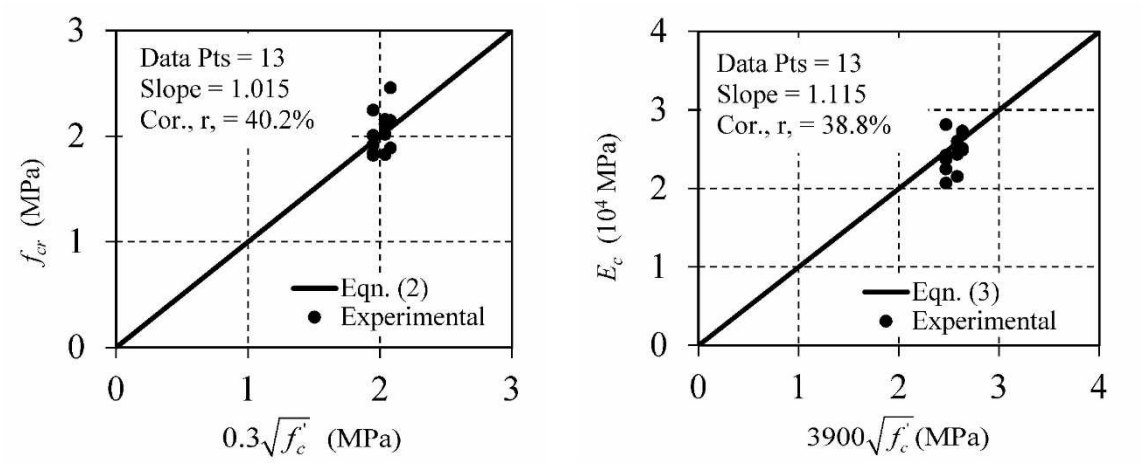

Fig. 3. Comparison between the test results and Eqn. (2) and (3)

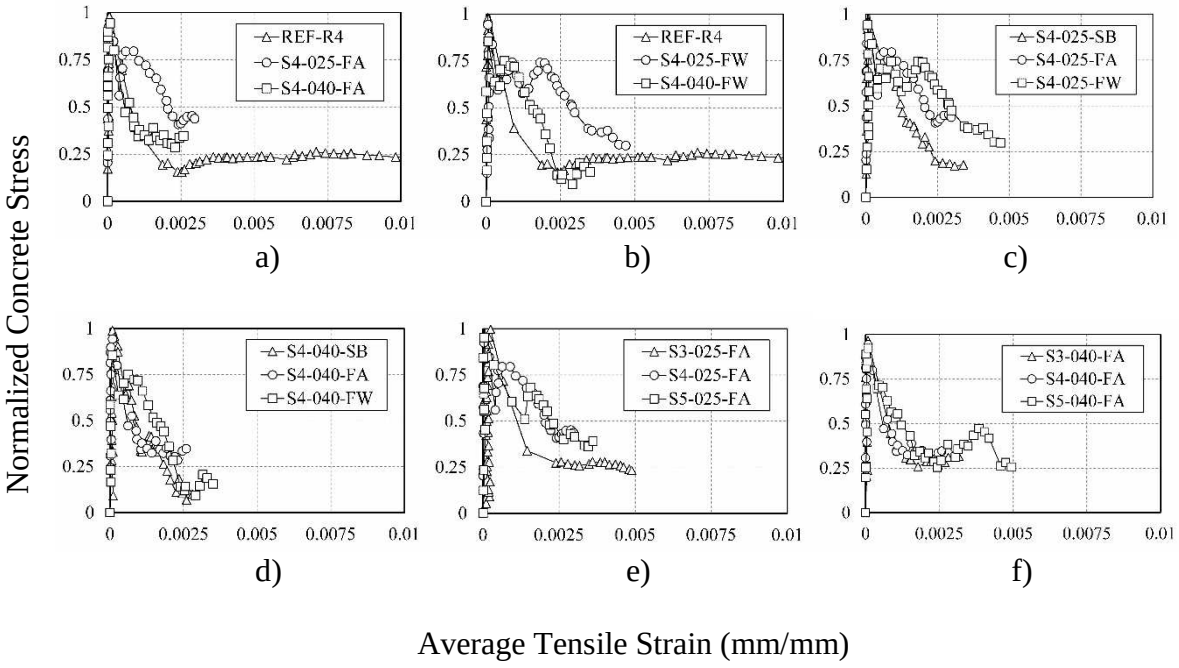

Fig. 4. Average stress strain curve of concrete

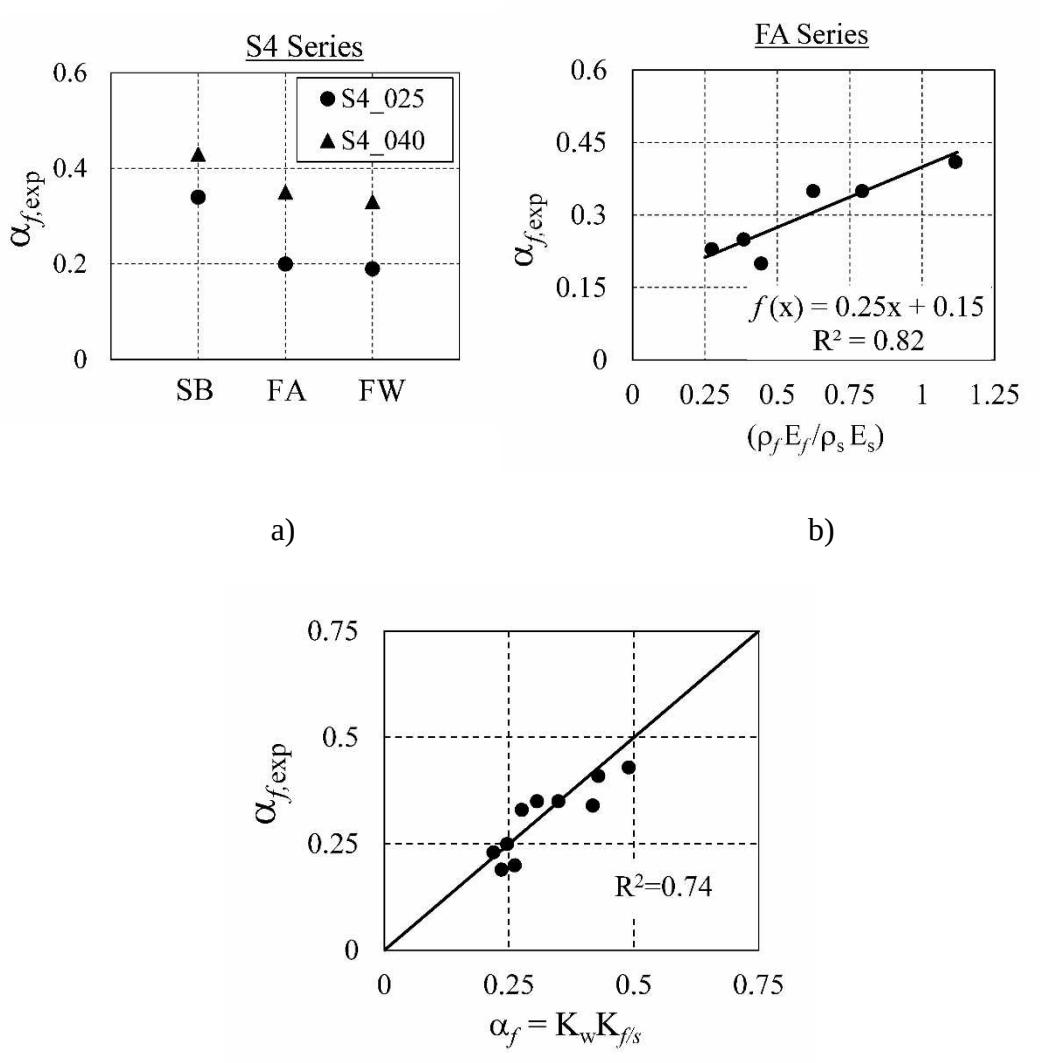

Fig. 5. Parameters studies of the tension stiffening equations

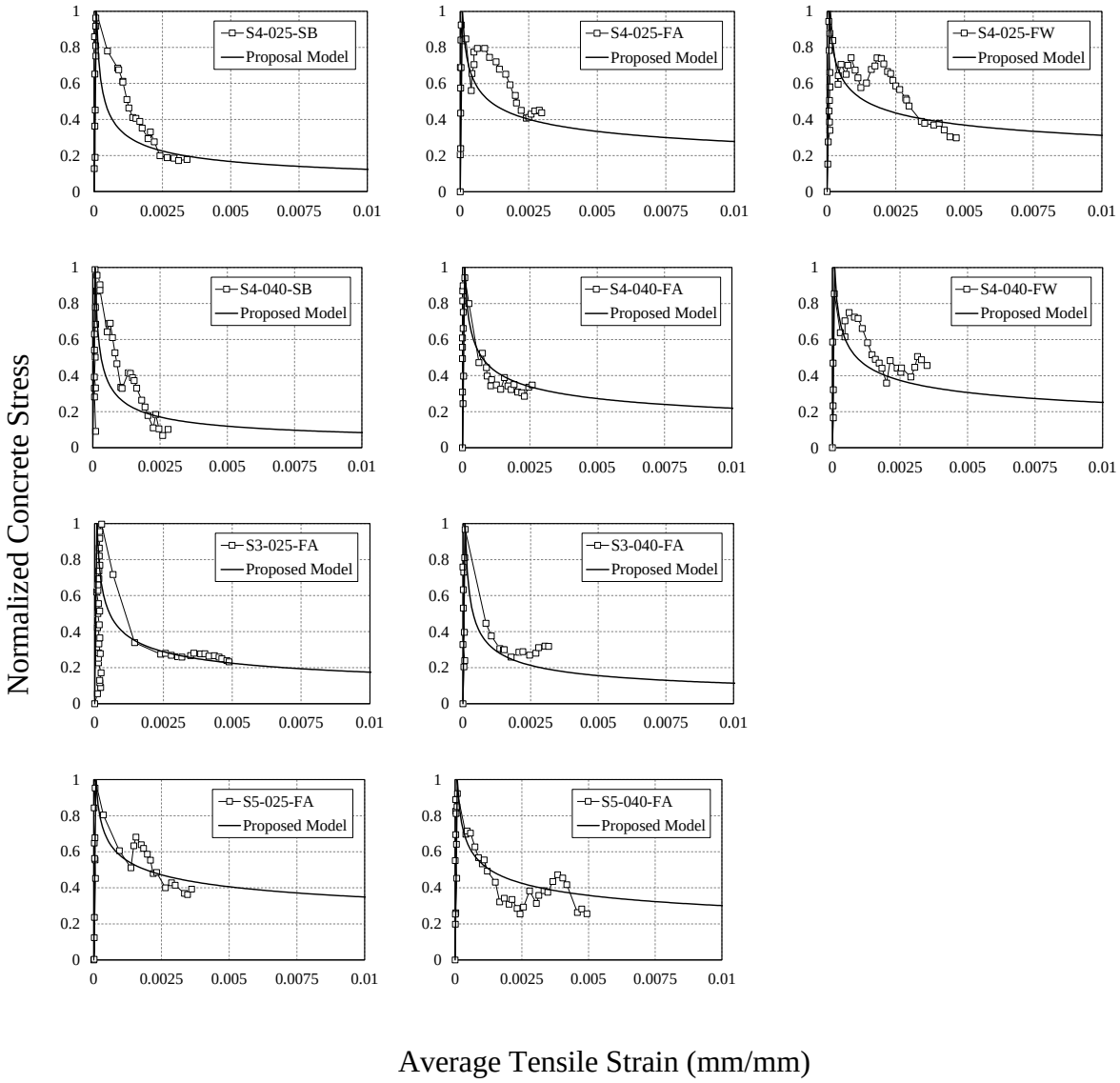

Fig. 6. Comprasion of the experimental results and Eqns. (10)-(14)

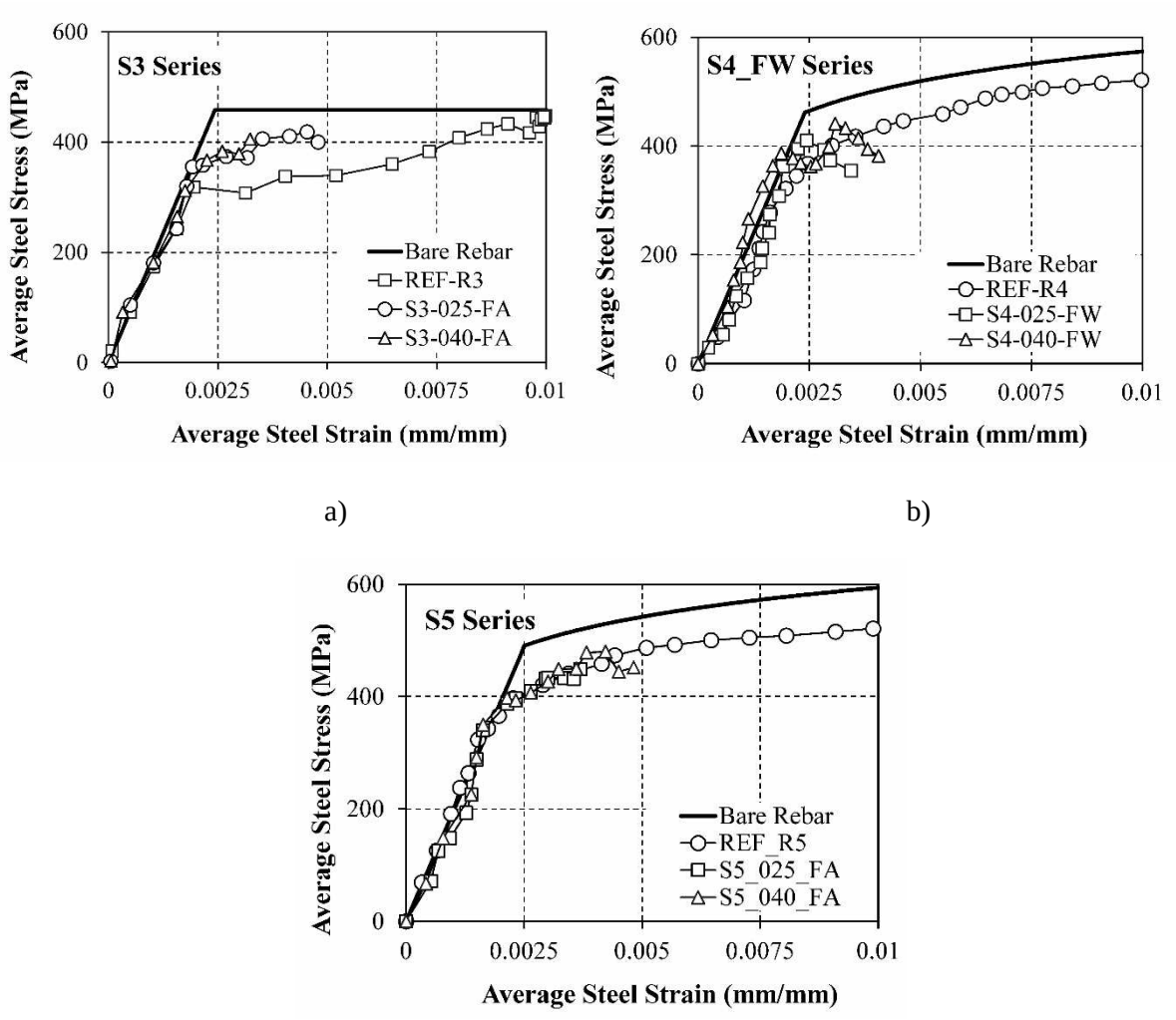

a) b)

c)

Fig. 7. Stress strain relationships of steel in the test

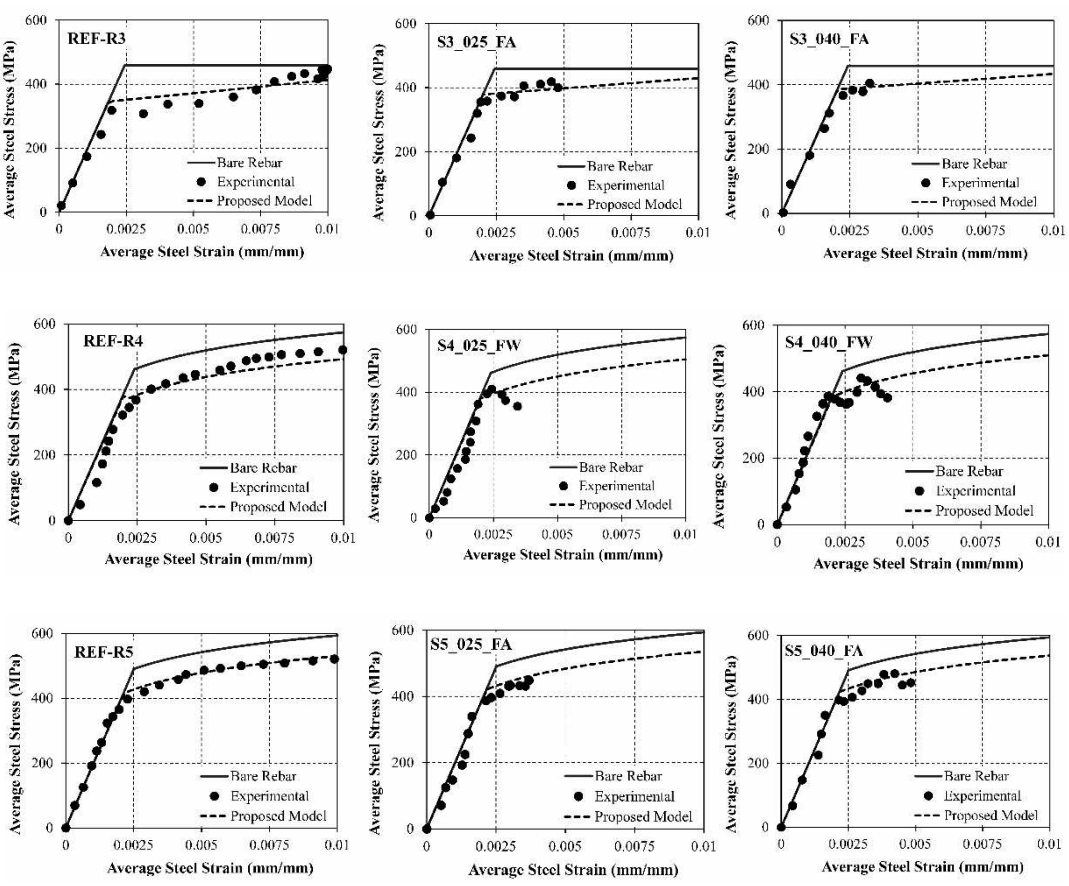

Fig. 8. Comparison of the stress strain relationships in steel

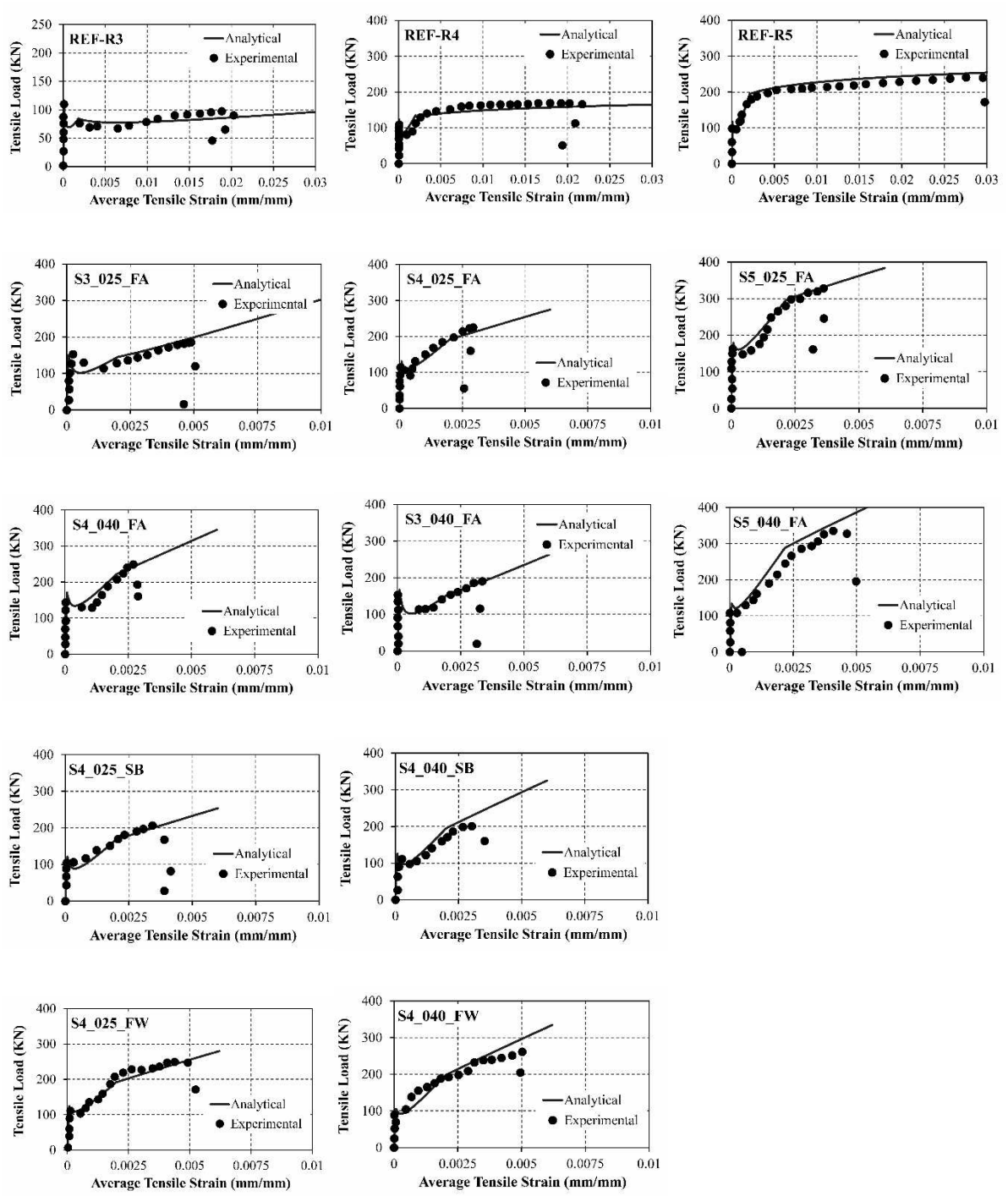

Fig. 9. Comparison of the load strain relationships

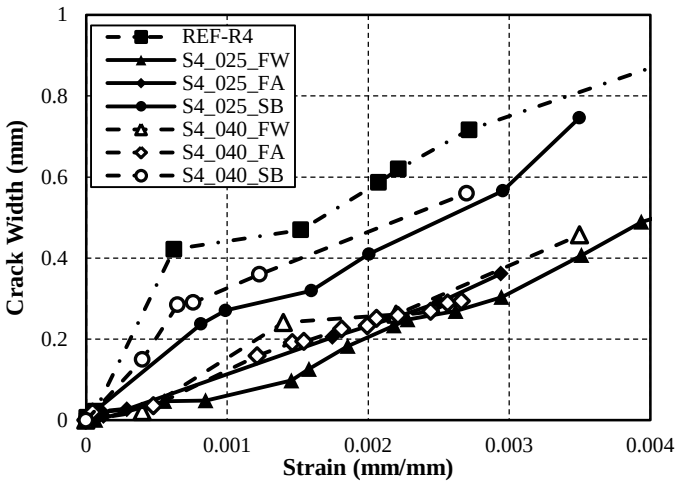

Fig. 10. Crack width details

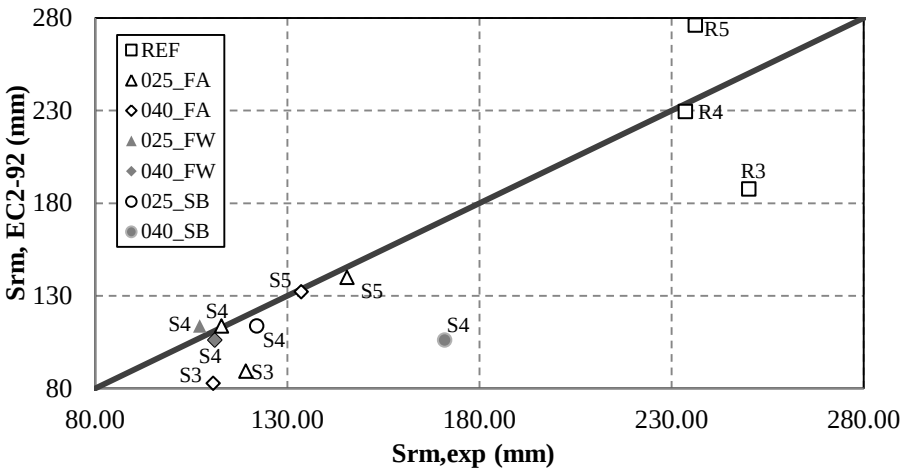

a)

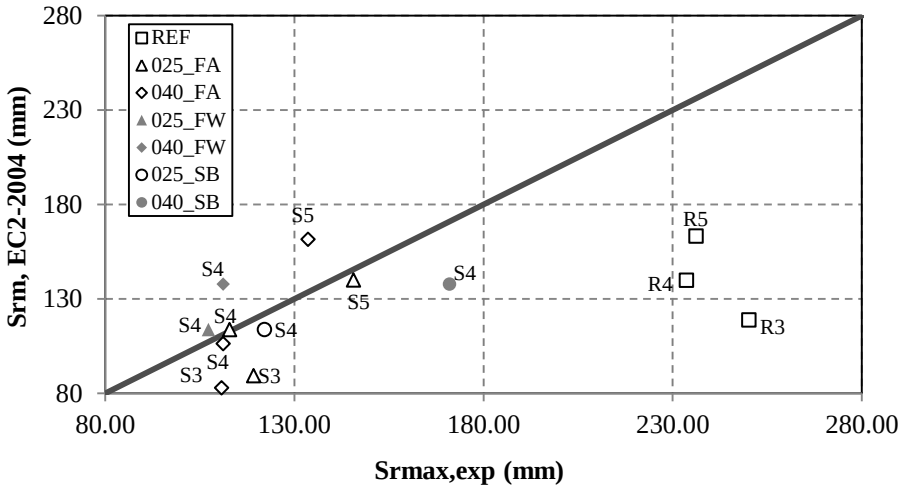

b)

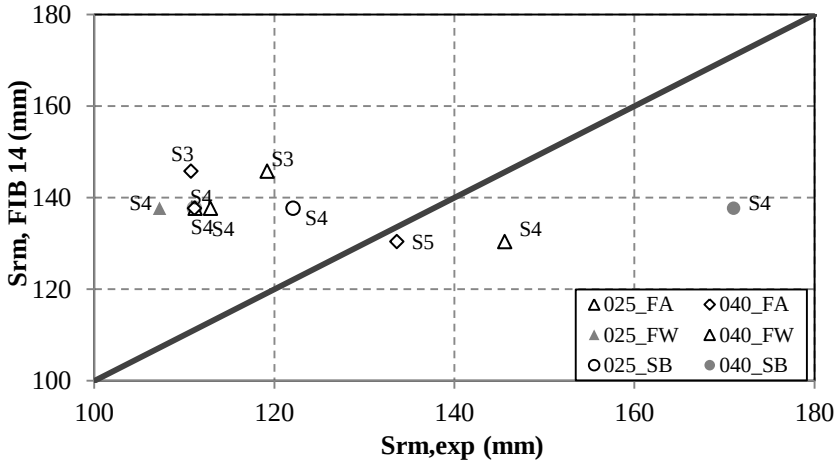

c)

Fig. 11. Comparison of experimental and code values of crack spacing:(a) EC2-92;(b) EC2-4;(c) fib14(2001)

Tables

Table 1. Summary of the Material Properties

Specimen Name	f_c' (MPa)	ρ_s (%)	f_{sy} (MPa)	E_s (GPa)	ρ_f (%)	f_{fu} (MPa)	E_f (GPa)	σ_p (MPa)	$\varepsilon_{c,sh}$ (μm/m)	$\varepsilon_{s,sh}$ (μm/m)
REF-R3	42	0.31	458	189	0	—	—	—	3	155
REF-R4	42	0.55	462	190	0	—	—	—	6	147
REF-R5	42	0.87	469	195	0	—	—	—	9	134
S3-025-FA	46	0.31	458	189	0.56	827	83	4.2	3	141
S3-040-FA	46	0.31	458	189	0.90	876	72	4.2	3	156
S4-025-FA	48	0.55	462	190	0.56	827	83	4.7	5	145
S4-040-FA	46	0.55	462	190	0.90	876	72	4.2	6	182
S5-025-FA	46	0.87	469	195	0.56	827	83	4.2	9	155
S5-040-FA	48	0.87	469	195	0.90	876	72	4.7	12	211
S4-025-SB	42	0.55	462	190	0.56	827	83	3.8	6	156
S4-040-SB	48	0.55	462	190	0.90	876	72	4.7	6	175
S4-025-FW	42	0.55	462	190	0.56	827	83	3.8	6	161
S4-040-FW	48	0.55	462	190	0.90	876	72	4.7	7	192

Table 2. Statistical Parameters of Code Guidelines and Experimental Results Comparison

Crack spacing	n	σ%	δ	σ_δ	R^2	r
S_{rm} (EC2-92)	13	19.42	0.89	0.16	0.67	0.86
S_{rm} (EC2-04)	13	24.97	0.88	0.22	-1.37	0.46
S_{rm} (fib 14)	10	21.39	1.12	0.17	-26.23	0.39